Polymer 54 (2013) 4045–4058

Contents lists available at SciVerse ScienceDirect

Polymer

journal homepage: www.elsevier.com/locate/polymer

Feature article

Poly(2,3-diphenyl-1,4-phenylenevinylene) (DP-PPV) derivatives: Synthesis, properties, and their applications in polymer light-emitting diodes

Jiun-Tai Chen*, Chain-Shu Hsu*

Department of Applied Chemistry, National Chiao Tung University, Hsinchu 30050, Taiwan

ARTICLE INFO

Article history:
Received 18 February 2013
Received in revised form
10 April 2013
Accepted 14 April 2013
Available online 23 April 2013

Keywords:
Polymer light-emitting diodes
Conjugated polymers
Fluorescence
Electroluminescence

ABSTRACT

Poly(1,4-phenylene vinylene) (PPV) has drawn a great deal of attention in the last two decades because of their applications in areas such as light-emitting diodes. To improve the solubility and optoelectronic properties, various PPV derivatives have been synthesized and investigated for their light-emitting performance. Among PPV derivatives, poly(2,3-diphenyl-1,4-phenylenevinylene) (DP-PPV) and its derivatives have been widely studied because of their promising electronic properties. Here, we review the synthesis, properties, and device performances of DP-PPV derivatives, which exhibit high external efficiency and brightness in polymer light-emitting diodes. For example, long alkyl chains were introduced to increase the solubility of DP-PPV. DP-PPV derivatives having liquid crystalline side groups were also synthesized and polarized emissions were obtained. In addition, bulky dendritic side groups were incorporated on the pendant phenyl ring and quantum efficiency of the device was significantly enhanced with increasing the generation of dendrons. By introducing methoxy or long branched alkoxy chains into DP-PPV, a maximum brightness of 78050 cd/m^2 with a low turn-on voltage of 4.0 V was also achieved by fabricating a multilayer electroluminescent device. In addition, the self-assembly behaviors and optical properties of different DP-PPV derivatives in solution and in confined environment are also discussed.

1. Introduction

Polymer light-emitting diodes (PLEDs) have attracted much attention in the last twenty years because of their applications in solid-state lighting, and large-area, flat-panel displays [1–8]. Among many promising conjugated polymers for PLEDs, poly(1,4-phenylene vinylene) (PPV) and its derivatives have been widely studied because of their high quantum yield and excellent thermal stabilities [9–13]. Light-emitting PPV films are most commonly synthesized from precursor polymers by high temperature annealing, due to their insolubility. To improve the solubility and the optoelectronic properties of PPV, a wide range of PPV derivatives have been synthesized and their light-emitting performance have been tested. For example, alkoxy groups are often introduced to the polymer backbone to improve the solubility in common organic solvents, as demonstrated in the well-known poly[2-methoxy-5-(2′-ethylhexoxy)-1,4-phenylenevinylene] (MEH-PPV) [14–17]. These modified PPV derivatives often have smaller energy gaps compared to the unmodified PPV because of the electron-releasing effect of the alkoxy groups [18].

Poly(2,3-diphenyl-1,4-phenylenevinylene) (DP-PPV) is among the most studied representatives in the PPV series. By using the Diels–Alder reaction, Hsieh et al. reported a chlorine precursor route (CPR) to synthesize DP-PPV [19–21]. As shown in Scheme 1, 1,4-bis(chloromethyl)-2,3-diphenylbenzene was polymerized with potassium *tert*-butoxide to give the chlorine precursor polymer of DP-PPV. DP-PPV with different degrees of conversion was obtained by thermally converting the chlorine precursor at different temperatures [22]. The degree of conversion was found to be a function of the heating temperature rather than the duration of the heating process. Higher PL intensity and lower photoconductivity (2-3 orders) were also observed for the fully converted DP-PPV than PPV [22].

The properties of DP-PPV have been studied by different techniques. For example, Lee et al. investigated the C 1*s* core level spectra and the valence band spectra for DP-PPV using X-ray photoelectron spectroscopy [23]. The core level peaks of DP-PPV were fitted to the bonding states of the carbon species. The surface topography of DP-PPV film coated on an indium-tin oxide (ITO) substrate was studied by Razafitrimo et al. using scanning tunneling microscopy [24]. DP-PPV was found to exhibit elongated bundles, and a closer look at

* Corresponding authors. Tel.: +886 3513 1523.
E-mail addresses: jtchen@mail.nctu.edu.tw (J.-T. Chen), cshsu@mail.nctu.edu.tw (C.-S. Hsu).

0032-3861
http://dx.doi.org/10.1016/j.polymer.2013.04.037

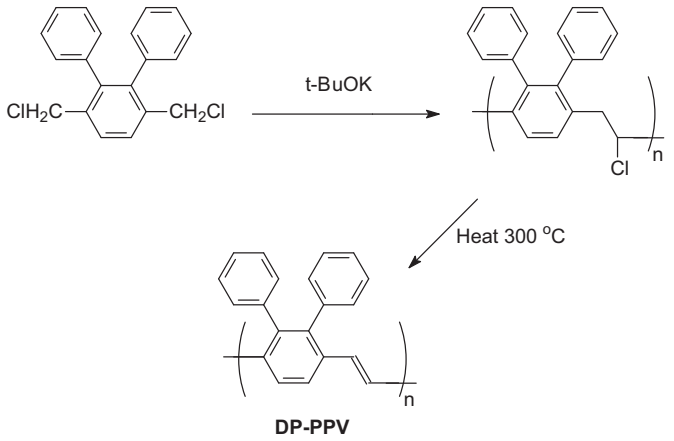

Scheme 1. Synthesis of DP-PPV by the chlorine precursor route.

the large bundles showed a fibrous-like structure. For PLED devices, bilayer structures were prepared by Antoniadis et al. for which an electron transporter and emitter, tris(8-hydroxyquinoline)aluminum (Alq_3), was thermally sublimed on the fully converted DP-PPV films followed by Mg deposition [25]. The device efficiencies of the bilayer ITO/DP-PPV/Alq_3/Mg device were observed to be improved more than 10 times than that of the single layer ITO/DP-PPV/Mg devices. Alq_3 was found to act the role of an efficient electron injector, resulting in the balance of electrons and holes. To further improve the DP-PPV based PLEDs, the interface formation between DP-PPV and metals such as Al and Ca was studied by Ettedgui et al. using near-edge x-ray-absorption spectroscopy [26]. They found that Al does not create new unoccupied states in DP-PPV, while new unoccupied states are formed for Ca deposition.

Although the chlorine precursor route can be applied to synthesize DP-PPV and other highly phenylated PPVs, other non-precursor routes have been developed to synthesize soluble DP-PPV derivatives. Hsieh et al. pioneered this work by developing a versatile synthetic methodology that involves two steps [27]. The first step is to synthesize substituted DP-PPV monomers via the Diels–Alder reaction. The second step is to polymerize the monomers via a modified Gilch route [27,28]. By applying this versatile method, monomers containing different functional substituents can be easily synthesized, and soluble DP-PPV derivatives with high molecular weights can be obtained [27–32]. Devices using DP-PPV derivatives containing fluorenyl or long branched alkoxy substituents with the configuration of indium tin oxide (ITO)/poly(3,4-ethylenedioxythiophene) (PEDOT)/polymer/Ca/Al has been fabricated and showed a high external quantum efficiency (3.39 cd/A), a low turn-on voltage (4.0 V), and a high brightness (16,910 cd/m^2) [29]. Better device performance was later achieved by using blade coating technique to fabricate multilayer electroluminescent device with the configuration of ITO/PEDOT:PSS/TFB/Polymer/TPBi/LiF/Al, where TFB is poly[(9,9-dioctylfluorenyl-2,7-diyl)-*co*-(4,4′-(N-(4-s-butylphenyl))diphenylamine)] and, TPBi is 1,3,5-tris(N-phenylbenzimi-dazol-2-yl) benzene. The maximum brightness of the device reached up to 78,050 cd/m^2 with a low turn-on voltage (4.0 V) and a high luminescence efficiency (10.96 cd/A) [33].

The advantages of DP-PPV derivatives are as follows: (1) synthesis of monomer and polymer is relatively easy, (2) the glass transition temperatures of the materials are high, (3) the fluorescence efficiency is high (65–85%), and (4) many possible molecular designs are available [7]. Here, we summarize the synthesis, properties, and their applications in PLEDs of several DP-PPV derivatives. For instance, liquid crystalline side groups can be incorporated into the polymer to produce polarized emissions [28,34]. Dendritic side groups can be introduced on the pendant phenyl ring to enhance the quantum efficiency [29]. Charge transport groups can also be integrated on the pendant phenyl ring to decrease the driving voltage of the devices [34]. In addition, we will discuss the photophysics, self-assembly behaviors, and confinement-induced property changes of DP-PPV derivatives. Finally, applications of DP-PPV derivatives in areas other than PLED will also be reviewed.

2. Synthesis and properties of DP-PPV derivatives

2.1. DP-PPV derivatives with long alkyl chains

The insoluble thin films of DP-PPV can be synthesized by a chlorine precursor route [22]. To improve the solubility of DP-PPV derivatives, Hsieh et al. reported the synthesis of a series of soluble DP-PPV derivatives [27]. The synthesis of the DP-PPV derivatives includes the synthesis of alkylated DP-PPV monomers via the Diels–Alder reaction, followed by the polymerization of the monomers via a modified Gilch synthetic route.

The synthesis of DP-PPV with long alkyl chains is shown in Scheme 2. The Diels–Alder reactions of 2,5-bis-(ethoxycarbonyl)-3,4-diphenylcyclopentadienone with 1-octyne, 1-decyne, or 1-dodecyne were carried out to produce 2a-c. These compounds were reduced with $LiAlH_4$ to give 3a-c, followed by reactions with $SOCl_2$ in methylene chloride to give monomer 4a-c. By applying a modified Gilch route using a nonpolymerizable acidic additive in the polymerization, soluble poly(2,3-diphenyl-5-hexyl-*p*-phenylene vinylene) (DP6-PPV), poly(2,3-diphenyl-5-octyl *p*-phenylene vinylene) (DP8-PPV), and poly(2,3-diphenyl-5-decyl-*p*-phenylene vinylene) (DP10-PPV) were obtained [27].

The UV-vis and photoluminescence (PL) spectra of DP6-PPV were also studied. The emission peak at 490 nm for DP6-PPV is around 10 nm blue-shifted compared with that of DP-PPV [35]. The blue-shifted spectra are caused by the steric effect of the *n*-hexyl group that decreases the effective conjugation length of the polymers. The PL quantum efficiency of DP6-PPV thin film reached 65%, one of the highest PL efficiencies for PPV derivatives. Such a high PL quantum efficiency from DP6-PPV may be attributed to the steric effect of the alkyl groups and the two phenyl rings. The self-quenching process by forming exciplexes or excimers was prevented because of the steric effect.

Huang et al. have also studied the coumarin terminated DP6-PPV [36]. They found that the coumarin terminated DP6-PPV has similar emission spectrum with that of DP6-PPV. But the photoluminescence efficiency of the coumarin terminated DP6-PPV ($\sim$0.78) is higher than that of DP6-PPV ($\sim$0.55). The PLED devices based on the coumarin terminated polymers (ITO/PEDOT/Polymers/Ba/Al) exhibited EL emission at 510 nm and a maximum brightness of 350 cd m^{-2} at 18 V with an external quantum efficiency of 0.04% at 61 mA cm^{-2}. This work provides a convenient way to modify DP-PPV derivatives by terminating, and the emission color and device performance can therefore be improved.

2.2. DP-PPV derivatives with liquid crystalline side groups

Linearly polarized emission has been desired for liquid crystal display (LCD) backlight applications. Many conjugated polymers with liquid crystalline side groups have been reported for polarized PLED application [37,38]. Li et al. have studied the synthesis DP-PPV derivatives with liquid crystalline side group [28,34]. A cyclohexylphenoxy or biphenyoxyl group was incorporated and served as the rigid mesogen core. An alkoxy or alkyl group was used as the flexible terminal and a methylene group was used as the spacer. These polymers were highly soluble and exhibited liquid crystalline behaviors [28].

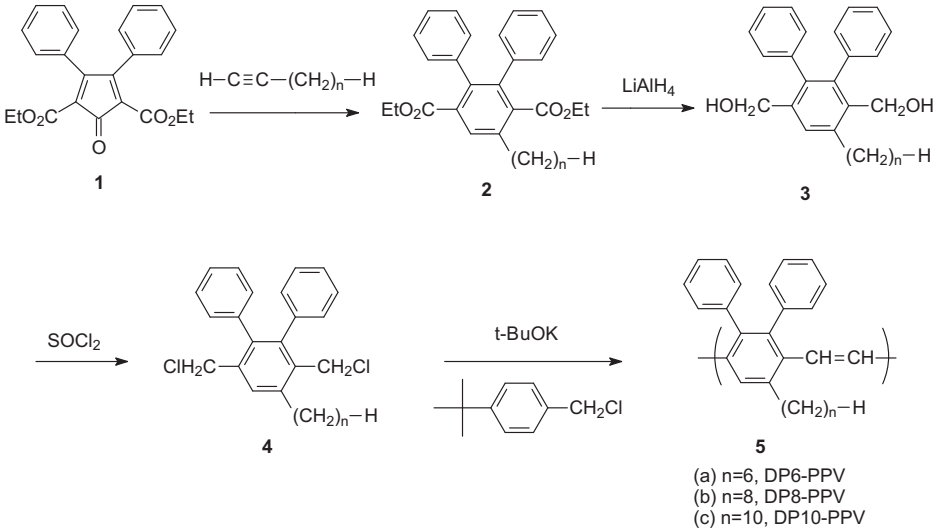

Scheme 2. Synthesis of DP-PPV with long alkyl chains.

The synthesis of DP-PPV with liquid crystalline side group is shown in Scheme 3. Similar to DP6-PPV, the synthesis of the monomer was begun with the Diels–Alder reaction. At first, 2,5-bis(ethoxycarbonyl)-3,4-diphenylcyclopentadienone (6) was reacted with 4-(*n*-heptyloxy)-4-(4-pentynloxy)biphenyl and 1-(4-pentylcyclohexyl)-4-(4-pentynyloxy)benzene to give 7a and 7b, respectively. After reduction by $LiAlH_4$, the corresponding dialcohol 8a and 8b were produced. 8a and 8b were then reacted with $SOCl_2$ in methylene chloride to produce monomers 9a and 9b, respectively. By using a large excess of potassium *tert*-butoxide in the absence of chain terminating agents, soluble 10a and 10b were synthesized without gelation.

These DP-PPV derivatives 10a and 10b were soluble in common organic solvents and showed strong photoluminescence (PL). Nematic liquid crystalline phases were shown in these DP-PPV derivatives. The absorption edges and the emission peaks of the thin films of these DP-PPV derivatives were found to be blue-shifted, caused by the liquid crystalline side group. Electroluminescence (EL) of the DP-PPV derivatives with liquid crystalline sides groups in single-layer devices was also examined. Polarized optical properties of these DP-PPV derivatives can be obtained by applying a rubbing treatment at a liquid crystalline state. As shown in Fig. 1, the dichroic PL spectra of the polymers indicated that the emitting light from the rubbed film was polarized perpendicular to the rubbing directions [30]. The liquid crystalline side groups were aligned along the rubbing directions, while the alignment of the polymer backbones was perpendicular to the rubbing directions (see Fig. 2). Therefore, relatively large absorption and emission were obtained in the orthogonal direction with respect to the rubbing direction. The dichroic ratio for these polymers was better than those for dialkoxy side chain liquid crystalline PPVs [39].

2.3. DP-PPV derivatives with dendritic side groups

For conjugated polymers, intermolecular interactions such as aggregation and excimer formation can greatly reduce the

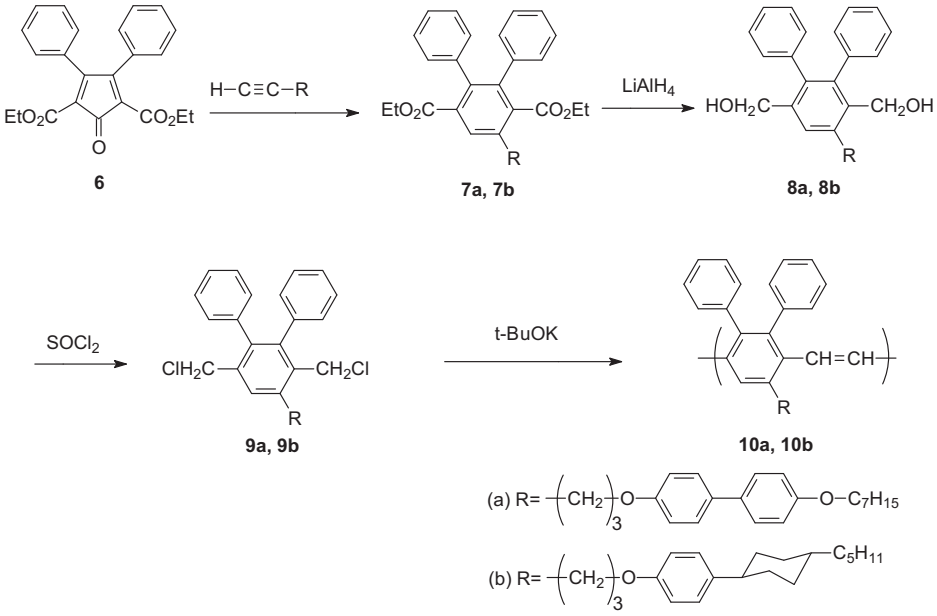

Scheme 3. Synthesis of DP-PPV with liquid crystalline side groups.

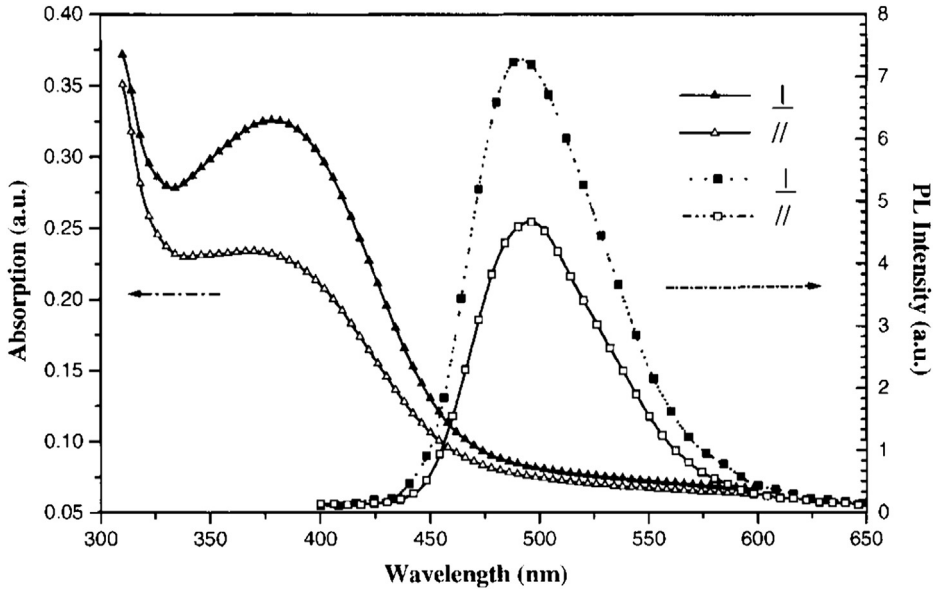

Fig. 1. Polarized optical absorption spectra and PL spectra of polymer 10a. Reproduced with permission from the literature [28].

luminescent quantum efficiency of the fabricated devices. To avoid such intermolecular interactions, a common strategy is by incorporating bulky dendritic side groups to the backbones of conjugated polymers. Different dendron-containing conjugated polymers have been synthesized and their properties have been studied [40–42]. Yang et al. reported the synthesis and characterization of DP-PPV containing dendron side groups [29]. Different copolymers from copolymerizing with 1,4-bis(chloromethyl)-2,5-dimethoxybenzene and 1,4-bis-(chloromethyl)-2-[4′-(3,7-dimethyloctoxy) phenyl]-3-phenylbenzene were synthesized and characterized.

The synthesis of dendrons is shown in Scheme 4. At first, (3,5-dihydroxyphenyl) methanol was added to a solution of 11-bromo-1-undecene, potassium carbonate, and potassium iodide in acetonitrile to produce compound 12. Then a solution of triphenylphosphine in THF was added to the solution of 12 and carbon tetrabromide in THF to produce 13. To a solution of 13, potassium carbonate, and 18-crown-6 ether in acetone, 3,5-dihydroxyphenyl methanol was added to obtain compound 14. By using 14 as the starting material and following the synthetic procedure for 13, compound 15 was synthesized. Finally, compound 16 was obtained by following the synthetic procedure for 14 and using 15 as the starting material [29]. Long alkenyl chains were introduced onto dendrons to increase the solubility. Terminal vinyl bonds were used to identify intermediates and monomers. The synthetic route for dendron-containing monomers G1M-G3M with different generations is outlined in Scheme 5. For example, to a solution of 12, 17, and triphenylphosphine (PPh3) in THF, diethyl azodicarboxylate (DIAD) was added to produce the monomers via dehydration [29].

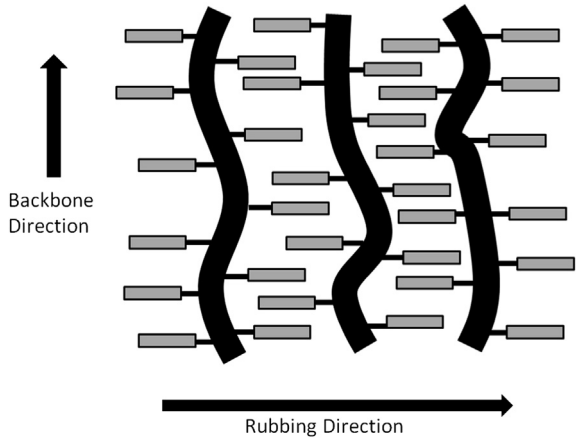

Fig. 2. The alignment of liquid crystalline side groups and polymer backbones by rubbing treatment. Reproduced with permission from the literature [28].

The polymerization was carried out via Gilch route to obtain soluble PPV derivatives. Only oligomers were synthesized during homopolymerization of Dendron-containing monomers. In addition, these oligomers did not have sufficient film-forming and thermal properties. Therefore, copolymerization was performed to effectively lower the steric hindrance during polymerization and to increase polymer molecular weights. The synthetic route for polymers from copolymerizing G1M-G3M with two other monomers 18, 19 is outlined in Scheme 6. For example, a mixture of G3M, 18, and 19 in THF was added with a solution of potassium *tert*-butoxide in THF. The incorporation of monomer 18 has been reported to increase the charge mobility inside the polymer layer [43]. The incorporation of monomer 19 has been studied to have electron-dominating properties [32]. Therefore, the incorporation of monomers 18 and 19 was used to adjust the electrical and optical properties of the synthesized polymers. Polymers with high molecular weights with relatively narrow polydispersities were obtained, and these polymers were soluble in common organic solvents [29].

The UV-vis absorption maxima of synthesized polymer thin films were examined and showed small red-shift compared with those in the solution state. The dendritic side groups were able to prevent the interchain interaction and aggregation. The PL quantum efficiency of synthesized polymers was studied and was found to increase with increasing the generation of dendrons. This result also implies that high generation dendrons can suppress the aggregation of polymer chains [29]. Therefore, the incorporation of dendritic group into polymers has the benefit of higher quantum efficiency and less chain aggregation, while keeping the emission color. The synthesized polymers were also used to fabricate double-layer light-emitting diodes with the configuration of ITO/PEDOT:PSS/Polymer/Ca/Al. The hole-injection ability and the device performance were both improved by introducing high-generation dendritic groups into polymers.

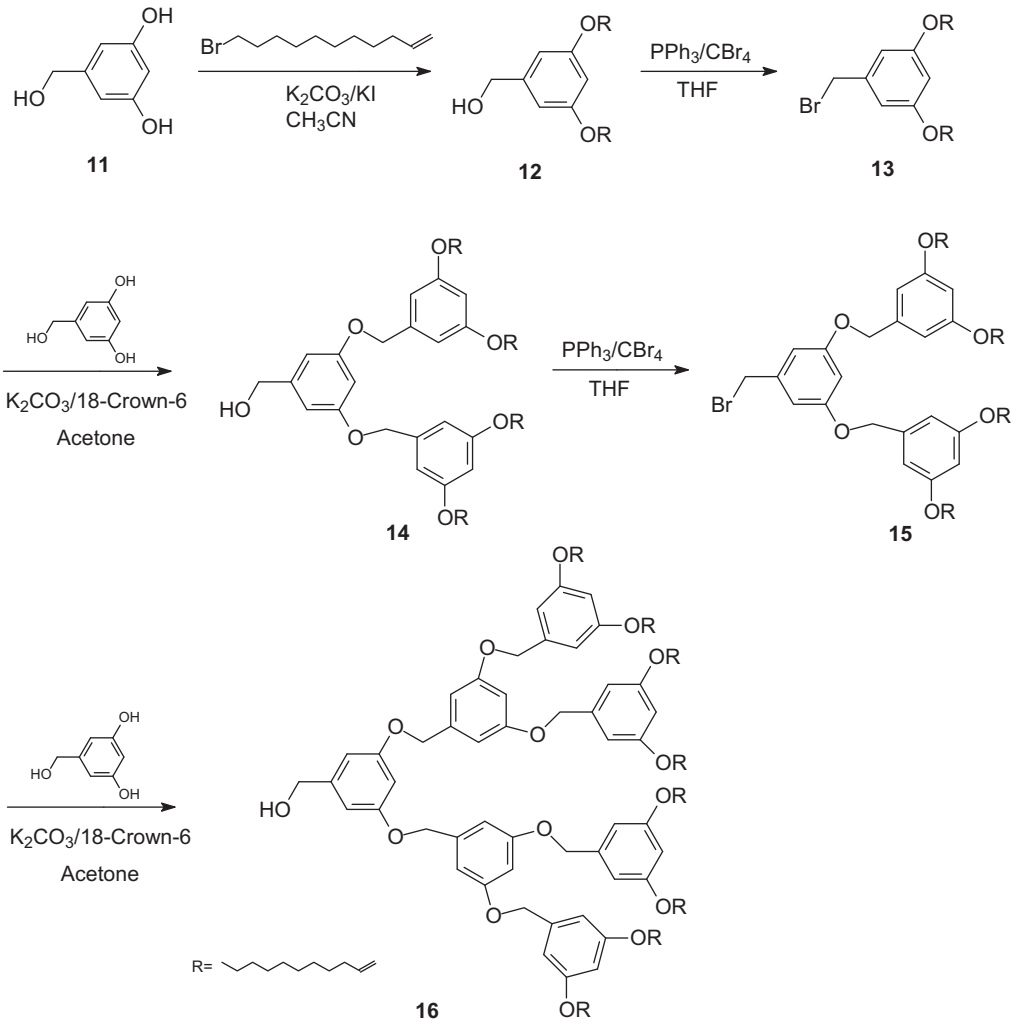

Scheme 4. Synthesis of dendrons.

2.4. DP-PPV derivatives with bulky charge transport groups

DP-PPV derivatives with bulky charge transport groups were also synthesized by Yang et al. [34] As shown in Scheme 7, compound 24 was prepared from condensation of benzyl, salicyladehyde, and aniline under acidic condition, followed by alkylation to give compound 25. After Diels–Alder reaction of compound 25 with 2,5-Bis(ethoxycarbonyl)-3,4-diphenylcyclopentadienone (26), compound 27 was obtained. Compound 27 was reduced by $LiAlH_4$ to produce compound 28 which later reacted with thionyl chloride to give monomer 29. Finally, polymerization of monomer 29 was carried out in the presence of large excess of potassium *tert*-butoxide.

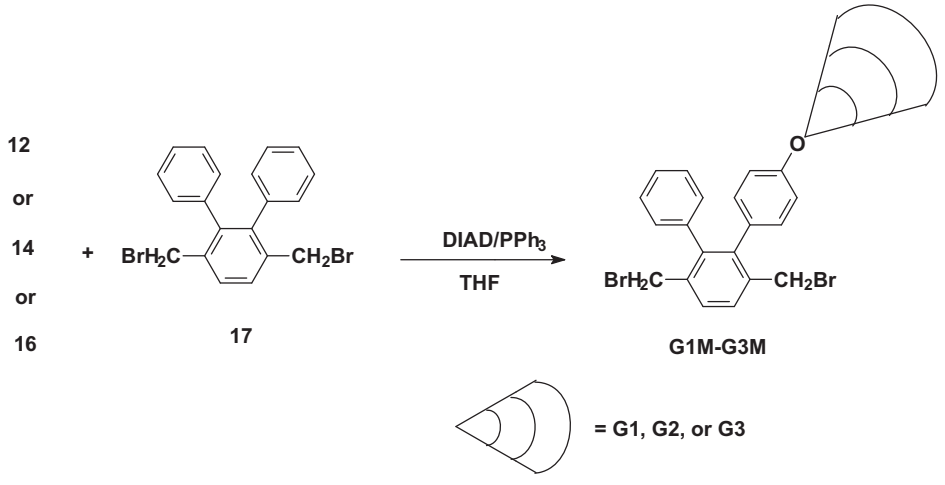

Scheme 5. Synthesis of dendron-containing monomers.

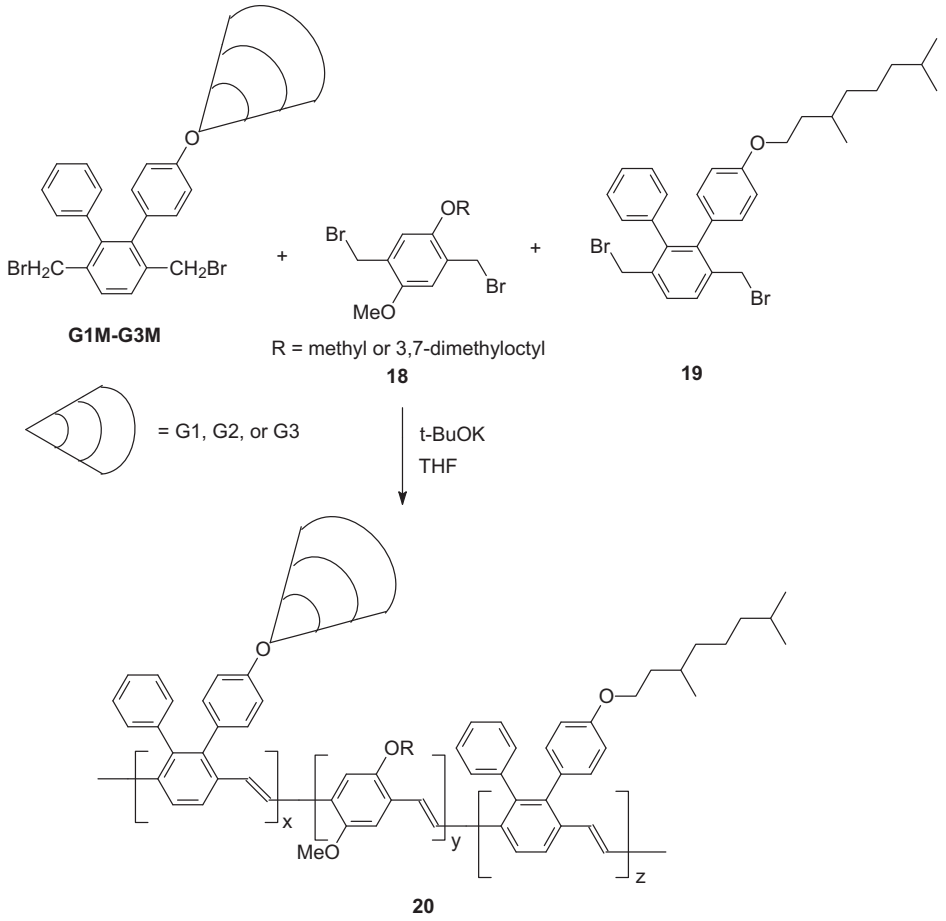

Scheme 6. Synthesis of dendron-containing DP-PPV derivatives.

The synthesized polymers were soluble in common organic solvents such as toluene, THF, and chloroform. The PL spectra of the polymers showed smaller red-shift between solid state and dilute solution, comparing with other PPVs such as MEH-PPV. This result demonstrated that the bulky side group can significantly reduce the aggregation of the polymer chains. The fluorescence quantum yield of the synthesized polymer was 0.65, comparing with the standard of quinine sulfate (ca. 1×10^{-5} M solution in 0.1 M H_2SO_4, with a fluorescence quantum yield of 55%). The quantum yield results also showed that the introduction of the bulky side group can increase the PL yield because the separation of the polymer backbones can prevent interchain exciton transfer [44]. The synthesized polymers were also fabricated as double-layer LED devices by using the configuration ITO/PEDOT:PSS/Polymer/Ca(Al). The blurish-green emission at 490 nm in the EL spectra is in good agreement with the PL emission. Therefore, EL and PL of the synthesized polymer are from similar excited states. The turn-on voltage of the device is 8 V with a maximum brightness of 22 cd/m^2 and maximum EL yield of 0.11 cd/A at 12 V. The lower turn-on voltage of the polymer may be caused by the introduction of the imidazole charge transport side group, which can increase the charge transport properties.

2.5. DP-PPV derivatives with methoxy or long branched alkoxy chains

DP-PPV derivatives with methoxy or long branched alkoxy chains were synthesized via the Gilch polymerization method [32,33]. As shown in Scheme 8, the different molar ratios of monomers 31, 32, and 33 were used to synthesize polymers 34a-34c. For monomer 31, the alkyl substituents were introduced to the phenyl ring of DP-PPV to avoid gelation and to improve the solubility of the polymers. Monomers 32 and 33 were incorporated to increase the carrier mobility of the polymer layer [43]. The feeding ratios of monomers 31, 32, and 33 were 90:0:10, 85:5:10, and 70:20:10 for copolymers 34a, 34b, and 34c, respectively. These copolymers were soluble in common organic solvents such as THF, toluene, and chloroform. The number-average molecular weights (M_n) were determined to be 3.1×10^5, 5.6×10^5, and 2.8×10^5 g/mol for copolymers 34a, 34b, and 34c, respectively.

Eight devices (A-H) were fabricated based on the synthesized copolymers, and the device performance was summarized in Table 1. For these devices, poly[(9,9-dioctylfluorenyl-2,7-diyl)-*co*-(4,4′-(N-(4-s-butylphenyl))diphenylamine)] (TFB) was used as the hole-transport layer (HTL) and as the electron blocking layer (EBL). For polymer 34a, a single layer device (device A) and two bilayer devices (devices B and C) were fabricated. The maximum brightness of device A was found to be 6138 cd/m^2 at 9 V with the corresponding current efficiency of 0.46 cd/A at 5.5 V [33]. The maximum luminance of device B was increased to 8926 cd/m^2 by introducing the hole-transporting TFB layer. This TFB layer also blocked electrons at the TFB/polymer interface. The efficiency of device C was further improved by incorporating the electron-transporting layer, TPBI, to the device, resulting in an efficiency of 10.96 cd/A at 5.5 V. The maximum luminance was 19,660 cd/m^2 for device C, a 3-fold larger than that of device A. Two devices (devices D and E) were fabricated based on polymer 34b. The turn-on voltages (V_{on}) for devices D and E were around 3 V. The maximum luminance of device D was 43160 cd/m^2 at 12 V, while device E which incorporated a TFB

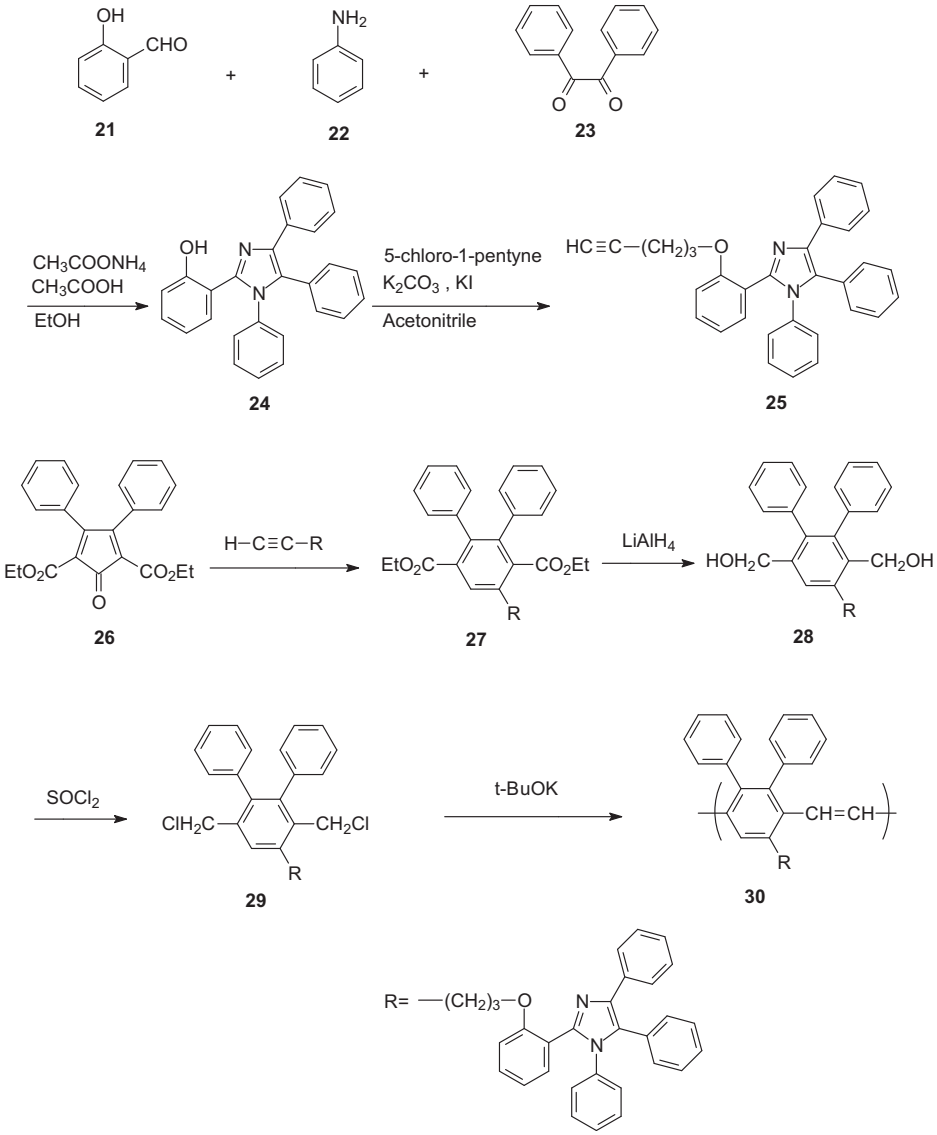

Scheme 7. Synthesis of DP-PPV derivatives with bulky charge transfer groups.

interlayer exhibited a maximum luminance of 72,179 cd/m^2 at 9.5 V [33]. By introducing monomer 32 into the main chain of polymer 34b, a better device performance was achieved, mainly because of the improved electron-transporting ability. Three devices (device F, G, and H) were fabricated based on polymer 34c. The turn-on voltages (V_{on}) of devices based on polymer 34c were about 4 V. For devices E and G, the maximum efficiency increased with the increasing feeding ratio of monomer 32 in the copolymers. As a result, device G showed improved device performance with a high efficiency of 9.15 cd/A at 4.5 V and a maximum luminance of 78,050 cd/m^2. These results demonstrated that these copolymers are excellent candidates for PLED applications.

2.6. Copolymers of DP-PPV derivatives with MEH-PPV

One of the most commonly used PPV based polymer is MEH-PPV. In order to study the possible color tuning of the PLED devices, there have been efforts to copolymerize MEH-PPV with DP-PPV derivatives. For examples, Chang et al. copolymerized MEH-PPV and DP6-PPV with different feeding ratios [45]. Utilizing these copolymers, bluish-green to orange light PLEDS on flexible polyethylene terephthalate) (PET) substrates were fabricated, with the emitted color tuned by the feeding ratio. The emitted color can be tuned according to the different feeding ratios, and the maximum EL intensity occurred when 50% of MEH-PPV was copolymerized.

Chiu et al. also copolymerized MEH-PPV and DP8-PPV via the Gilch route [46]. The chain compositions of the copolymers and the reactivity ratios of the monomers were calculated by ^{1}H NMR spectroscopy. They found that MEH-PPV and DP8-PPV monomers formed alternative copolymers as the feed ratio of the monomers were close to one-half. The ultraviolet–visible absorption spectrum of the alternative copolymer film was broader than those of copolymer films with other compositions, because the MEH-PPV attract like units from the adjacent chains during the film forming process [46].

2.7. DP-PPV derivatives with an inorganic core

Although DP-PPV derivatives are widely used for the application of OLED, the device performance of these derivatives is usually limited by the stability. Therefore, hybrid structures having an inorganic core are sometimes used to improve the stability or even to enhance the electroluminescence properties of the devices.

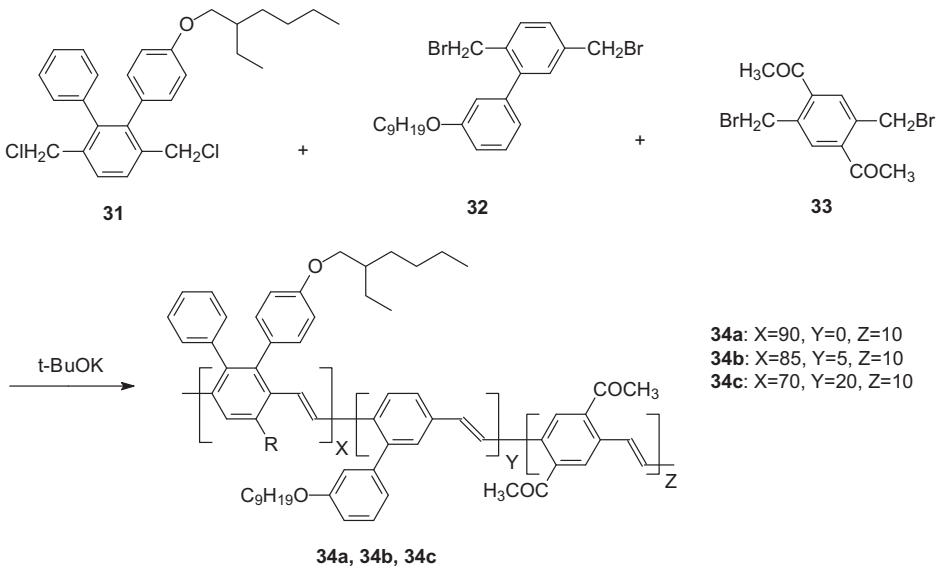

Scheme 8. Synthesis of DP-PPV derivatives with methoxy or long branched alkoxy chains.

Renaud et al. studied the device performance using a hybrid emitting material composed of poly(2,3-diphenyl-1,4-phenylenevinylene) (DP-PPV) and polyhedral oligomeric silsesquioxanes (POSS) as an inorganic core (POSS-DP-PPV) [47]. The trap states in POSS-DP-PPV based device was investigated by using the charge-based deep level transient spectroscopy (Q-DLTS) technique [48]. The analyses of the Q-DLTS spectra indicated that there are at least six types of traps present in the device. The mean activation energies of these traps are distributed in the range 0.3–0.5 eV within the band gap of the hybrid sample. The trap states with a large capture cross section might be originated from the inorganic part of hybrid sample, while those with smaller capture cross-section might be related to the organic part.

3. Self-assembly of DP-PPV derivatives in solution

The photophysical properties of DP-PPV derivatives are strongly affected by their structures, chain conformation, and self-assembly behavior of the polymer chains. The polymer chains can undergo self-assembly not only in the bulk state, but also in the solution state. DP-PPV based conjugated polymers are composed of semirigid backbone. These types of polymers usually undergo interchain aggregation in the solution state, as observed by spectroscopic studies. Many attempts have been made to further understand the interchain interaction in solution by techniques such as small-angle X-ray scattering (SAXS), small-angle neutron scattering (SANS), or dynamic light scattering (DLS) [18,49–52].

Table 1
Device performance of device A-H based on DP-PPV derivatives with methoxy or long branched alkoxy chains.

(Device no.) Device structure	EL λ_{max} (nm)	V_{on} (V)	L_{max} (voltage/V) (cd m^{-2})	Efficiency (B/V) (cd A^{-1})
(A) ITO/PEDOT:PSS/Polymer 34a/Ca/Al	552	3.0	6138 (9.0)	0.46 (5.5)
(B) ITO/PEDOT:PSS/TFB/Polymer 34a/Ca/Al	548	3.0	8926 (9.0)	1.0 (5.0)
(C) ITO/PEDOT:PSS/TFB/Polymer 34a/TPBI/LiF/Al	548	5.0	19,660 (12.5)	10.96 (5.5)
(D) ITO/PEDOT:PSS/Polymer 34b/CsF/Al	548	3.0	43,160 (12.0)	6.58 (3.0)
(E) ITO/PEDOT:PSS/TFB/Polymer 34b/CsF/Al	548	3.0	72,170 (9.5)	6.29 (4.0)
(F) ITO/PEDOT:PSS/TFB/Polymer 34c (N2)/CsF/Al	544	4.0	34,430 (9.5)	3.68 (5.0)
(G) ITO/PEDOT:PSS/TFB/Polymer 34c/CsF/Al	548	4.0	78,050 (10.5)	9.15 (4.5)
(H) ITO/PEDOT:PSS/TFB/Polymer 34c/TPBI/LiF/Al	544	4.0	20,870 (13.5)	7.96 (6.0)

3.1. DP6-PPV and DP10-PPV in solution

To study the possible mechanism of interchain aggregation of semirigid conjugated polymers, Li et al. first investigated the aggregation behavior of poly(2,3-diphenyl-5-hexyl-1,4-phenylenevinylene) (DP6-PPV) dissolved in chloroform and toluene of different qualities [49]. Chloroform is a relatively good solvent for DP-PPV, and toluene is a relatively poor solvent. By using dynamic light scattering (DLS), DP6-PPV was demonstrated to undergo interchain aggregation in both solvents, and the hydrodynamic radii of the aggregates were observed to be several micrometers. Fig. 3 shows the distribution of hydrodynamic radius R_h in the 1.0 wt% chloroform and toluene solutions at 25 °C. Three peaks are observed in the R_h profile. The largest R_h associated with the slow mode may be attributed to the average hydrodynamic radius of the aggregates in the solution. The two small peaks may be attributed to the internal relaxation mode of the networks and the motions of the rodlike segments in the aggregates.

Small-angle neutron scattering (SANS) was also utilized to characterize the conformational structure and aggregation behavior of DP6-PPV in solutions [49]. The SANS profiles demonstrate that the aggregation generated relative large network aggregates with the mass fractal dimension of 2.2–2.7. When the polymer is dissolved in chloroform, the highly stable segmental association of the polymer chains was attributed to the π–π complex present in the DP6-PPV powder. The stable complex was able to tie the polymer chains to form network aggregates in chloroform. Two power-law regimes were observed in the SANS profiles, which were associated with the mass fractal dimension of the networks and the rodlike subchains between the junction points for the polymer chains. When the polymer was dissolved in toluene, the poor affinity of the aliphatic side chains of DP6-PPV to the solvent caused further segmental association of the polymer chains. The SANS profiles revealed that the resultant aggregates

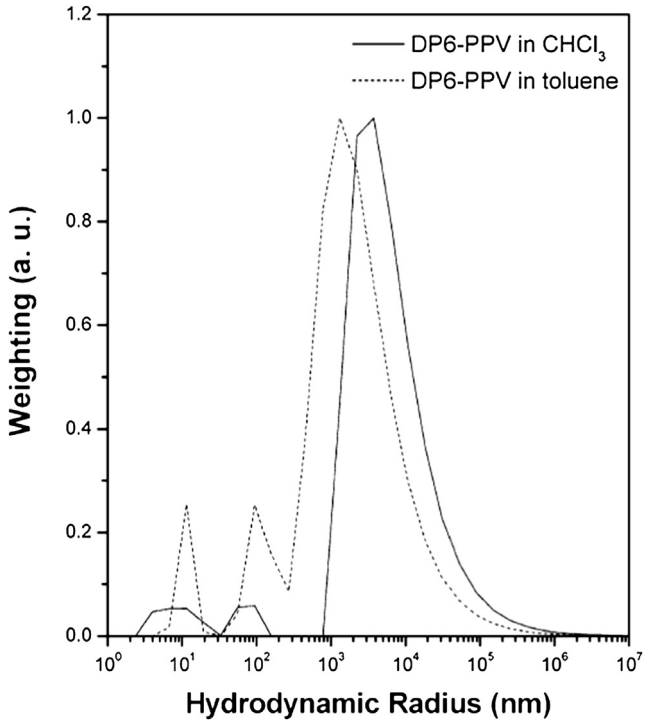

Fig. 3. The distribution of hydrodynamic radius R_h in chloroform and toluene solutions at 25 °C. Reproduced with permission from the literature [49].

were highly compact and the small average distance between the junction points resulted in the shift of the q^{-1} power-law regime. The aggregates of DP-PPV chains in toluene were identified as two different types of segmental associations with distinct stability, including the highly stable π–π complex and the micelle-like segmental association [49].

In addition to DP6-PPV, Li et al. also investigated the aggregation behavior and conformational behavior of poly(2,3-diphenyl-5-decyl-1,4-phenylenevinylene) (DP10-PPV), a PPV derivative with longer decyl side chain [50]. DP10-PPV was shown to have a weaker tendency toward aggregation than DP6-PPV does, because of the stronger steric hindrance of the side chain. But DP10-PPV chains still aggregate in semidilute solutions and form aggregates with the hydrodynamic radii of submicrometer to 10 μm in size. Different from the stable π–π complexes formed in DP6-PPV, the aggregates in DP10-PPVare loosely bound by the micelle-like association of chain segments that can be easily disintegrated by moderate heating. Fig. 4 shows the light scattering intensity of 0.5 wt % DP10-PPV in toluene at different temperatures [50]. The scattering intensity increases rapidly with the temperature, but the amplitude of the slow mode of the R_h distribution decreases significantly and the R_h values become lower. Therefore, the longer decyl side chain imposes a strong steric hindrance that can prevent the effective in-place stacking of the polymer chains.

3.2. Amphiphilic DP-PPV graft copolymers in solution

Interesting self-assembly behavior is expected if the rigid rodlike conjugated backbone is attached covalently to a coil segment. Liao et al. studied the self-assembly behavior of an amphiphilic hairy-rod DP-PPV copolymer composing of a hydrophobic poly(phenylene vinylene) backbone and hydrophilic poly(ethylene oxide) (PEO) side chains [51]. PEO is a water-soluble polymer and was attached to the DP-PPV backbone to produce amphiphilic copolymers. The self-assembly of the amphiphilic DP-PPV copolymers in both polar and non-polar solvents were investigated using small-angle X-ray scattering (SAXS). The structure of the amphiphilic copolymers in solution was affected by the solvent quality and the polymer concentration. THF is a relatively good solvent for DP-PPV and a moderately good solvent for PEO, while water is a non-solvent for DP-PPV and a good solvent for PEO. The polymers were relatively well dispersed in THF with some degree of aggregation. Different from THF solution, the amphiphilic polymers self-organized into cylindrical micelles in aqueous solutions. The aggregation number of the micelles was found to increase with increasing concentration.

3.3. Computer simulations of DP-PPV derivatives in solution

To further understand the conformational structures of DP-PPV derivatives in solution, computer simulations have also been employed to validate the experimental results of neutron or light scattering. Lukyanov et al. reparametrized atomistic and coarse-grained models for solvated DP-PPV derivatives by using quantum-chemical calculations and structure-based coarse-graining, respectively [52]. In their work, atomistic simulations were used to calculate the polymer–polymer solvent-mediated interaction potentials, and the solvent quality can be estimated. They confirmed the experimental evidence that both chloroform and toluene are good solvents for DP6-PPV and DP10-PPV. This conclusion is based on the alkyl side chain stretching, the backbone orientational correlations, and the potential of mean force of polymer dimers in the solvent. In addition, a coarse-grained model was used to study the persistence length and static structure factor of dilute solutions of DP6-PPV and DP10-PPV in chloroform and toluene.

4. Photophysics of DP-PPV and DP-PPV derivatives

In order to understand the optoelectronic properties of DP-PPV derivatives and to improve the device performances, the crystal structures and molecular packing of different DP-PPV derivatives have been studied [53,54]. Additionally, it is critical to understand the photophysical properties of DP-PPV derivatives for improving device performances. Time resolved photoinduced absorption and stimulated emission measurements have been applied for this purpose.

4.1. Photophysics of DP-PPV derivatives in film

Dogariu et al. studied the photophysics of DP6-PPV based on time resolved photoinduced absorption and stimulated emission measurements with temporal resolution of approximately 100 fs [55]. They showed that the emissive properties of DP6-PPV are fully consistent with a simple “four-level model”, in contrast to studies on other semiconducting polymers. In the four-level model, the system relaxes within the 100 fs temporal resolution to the lowest energy excited state, once the polymer is excited. The excited state population then decays in time by both radiative and nonradiative processes. The stimulated emission of the excited state spectrum of DP6-PPV is essential identical as the photoluminescence spectrum. To study the time decay of the excited state, single-wavelength measurements were performed with much higher sensitivity. The stimulated emission time decay is found to be the same as the photoluminescence time decay [55]. One important result of this study is that there is no significant photoinduced absorption in the stimulated emission spectral region. This result is reasonable because the photoinduced absorption spectrum depends on the energy distribution of the higher lying state, whereas the emission spectrum depends on the energy of the first excited state. Therefore, the absence of spectral overlap between the photoinduced absorption and emission in DP6-PPV is expected.

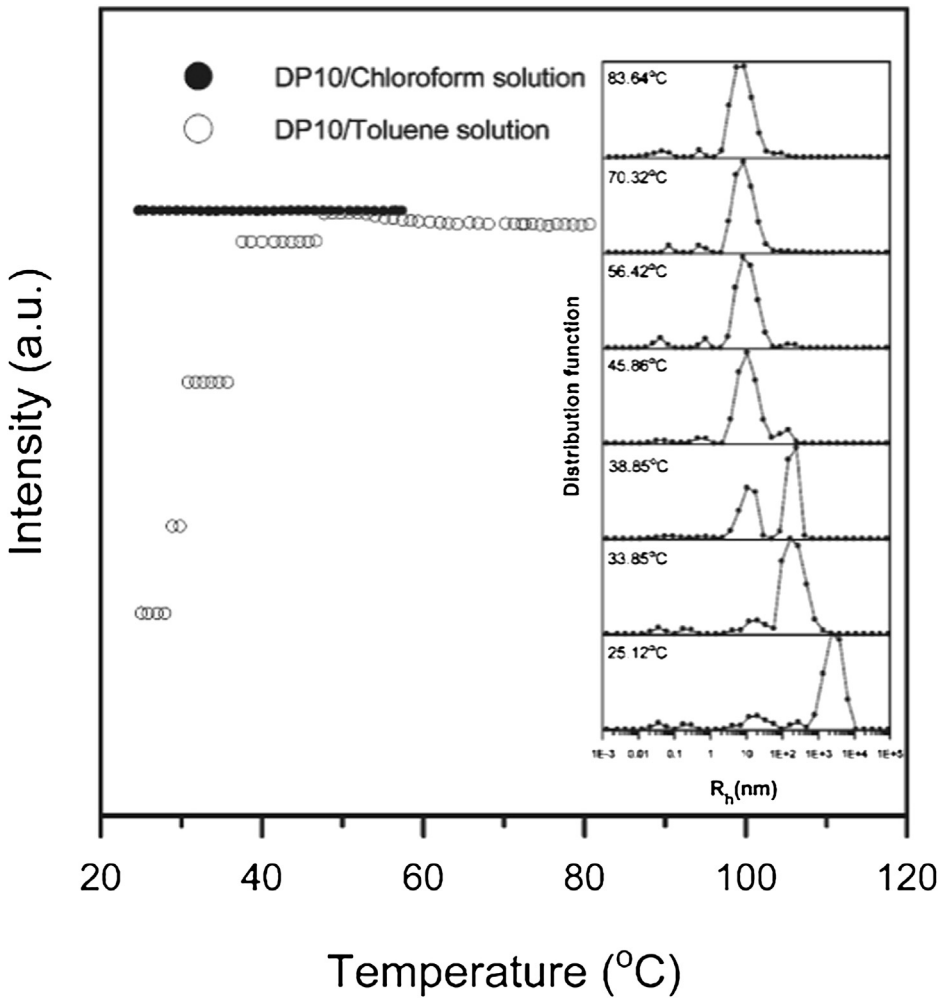

Fig. 4. Light scattering intensity of 0.5 wt % DP10-PPV in toluene at various temperatures. Inset is the corresponding R_h profile. Reproduced with permission from the literature [50].

4.2. Photophysics of DP-PPV derivatives in the presence of an electric field

The photophysical properties of conjugated polymers can be significantly affected by applying an electric field. The effect of electric field on the photophysics of DP-PPV derivatives was studied by Mehata et al. [56] They investigated the electric field modulation spectroscopy of DP6-PPV. The electroabsorption (E-A) spectra, electrophotoluminescence (E-PL) spectra, electrophotoluminescence excitation (E-PL-Ex) spectra, and field-induced change in PL decay profile were measured. The measurement of the E-A and E-PL spectra provided information of two basic properties of the polymer molecules, including the difference in molecular polarizability and the difference in electric dipole moment between the initial and final electronic state of transitions.

In DP6-PPV, two distinct effects were observed after applying an electric field, including the Stark shifts and the decreased PL intensity. The Stark shifts were observed in the absorption and PL spectra, which were caused by the change in polarizability and in dipole moment. The absorption and E-A spectra of DP6-PPV embedded in poly(methyl methacrylate) (PMMA) are shown in Fig. 5 [56]. E-A spectra were measured with the electric field strengths of 0.2–0.8 MV cm^{-1} at the magic angle of $\chi = 54.7^{\circ}$ and at the standard incidence angle of $\chi = 90^{\circ}$. The results of the polarized E-A spectra measured at $\chi = 54.7$ and 90° were almost identical, indicating that the isotropic distribution was maintained when DP6-PPV was embedded in the PMMA film. When the external electric field is applied, the molecular energy levels of the conjugated polymer were shifted, resulting in the shift or broadening of the optical spectra. The absorption spectrum was reproduced with three Gaussian bands, as shown in Fig. 5. In addition, a linear combination of the zeroth, first, and second derivatives of the Gaussian band (G1) with the lowest energy was used to simulate the E-A spectrum.

5. Polymer chains of DP-PPV and DP-PPV derivatives under confinement

The properties of polymer chains of DP-PPV and DP-PPV derivatives under confined environment have also been studied [57,58]. When polymer chains are confined in channels from alumina or block copolymer templates, optical and electrical properties which are different from the bulk can be observed.

5.1. DP-PPV chains absorbed to porous alumina

Qi et al. investigated the time-integrated and time-resolved optical properties of DP-PPV adsorbed to nanoporous alumina [57]. Nanoporous alumina is commonly used as templates for preparing polymer nanostructures [59,60]. The alumina membranes were first immersed in a solution of DP-PPV precursor polymers in tetrahydrofuran (THF). The polymer that was not adsorbed was removed by immersing the sample into a vial containing THF. The DP-PPV

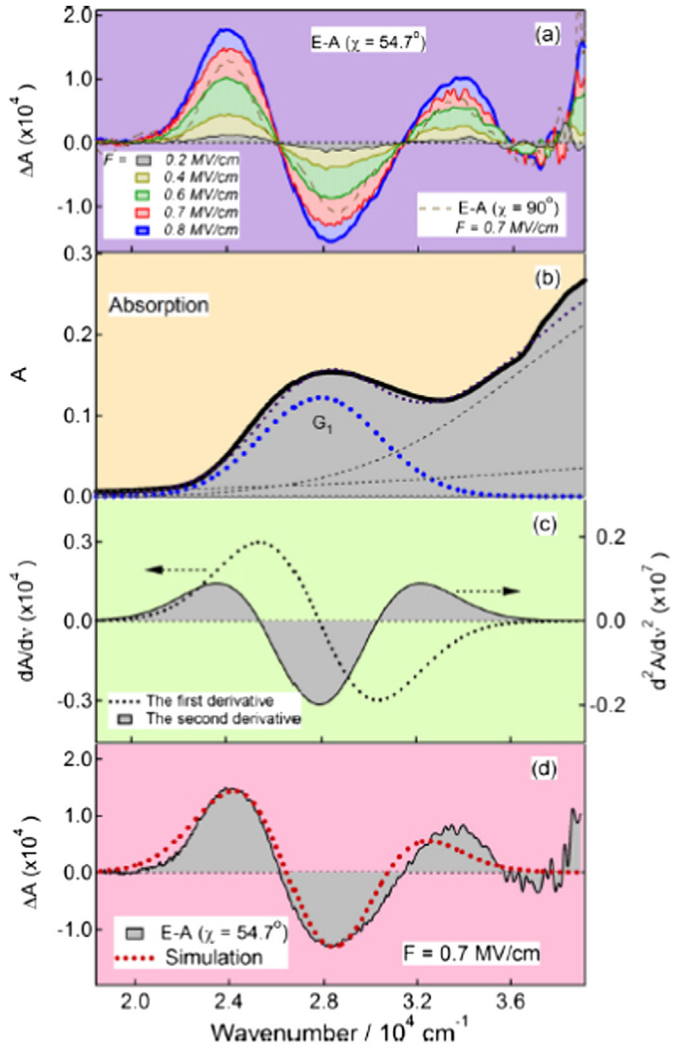

Fig. 5. (a) Electroabsorption (E-A) spectra of DP6-PPV in a PMMA film. (b) Absorption spectrum of DP6-PPV in a PMMA film. The decomposed Gaussian band (G1) with the lowest energy and two other Gaussian bands are also shown. (c) First and second derivative spectra of the G1 band. (d) Simulated E-A spectrum (red dotted line) and the observed spectrum (black shaded line). Reproduced with permission from the literature [56].

samples were then converted to the conjugated form after heating in a 280 °C for 2 h under vacuum [57].

Qi et al. studied the difference of the time-integrated photoluminescence spectra between alumina-adsorbed DP-PPV and bulk at 77 K, and substantial effects because of the confined environment were observed. As shown in the normalized PL spectra (see Fig. 6), there is a significant blue shift (0.068 eV) for the alumina-adsorbed samples [57]. In addition, the relative intensity of the 0-1 transition peak to the 0-0 transition peak of the alumina-adsorbed samples increases, and the peaks are broader. For the time-resolved experiments, same techniques were performed for both the bulk DP-PPV and alumina-adsorbed DP-PPV [61]. It was found that the effect of the adsorption on the fast decay dynamics of the optical excitation can be negligible. They concluded that the interactions of the DP-PPV chains with the alumina pore walls do not affect the intrachain dynamics on subnanosecond time scales. Still, the observed changes in the time-integrated photoluminescence spectra of DP-PPV can lead to significant possibilities for modifying the optical emission properties of DP-PPV derivatives by absorbing the polymers on alumina surfaces.

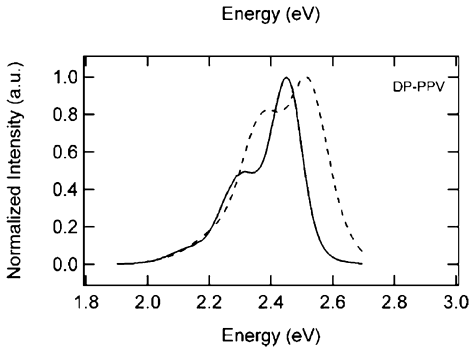

Fig. 6. Normalized PL spectra of DP-PPV at 77 K for bulk (solid line) and alumina-adsorbed (dashed line) samples. The excitation energy is 3.10 eV. Reproduced with permission from the literature [57].

5.2. DP-PPV derivatives in block copolymer templates

Nanoporous templates can also be prepared by the self-assembly of block copolymers [62,63]. Lo et al. studied the pore-filling process of poly(2,3-diphenyl-5-(trimethylene-octa(oxyethylene)-methoxy)-phenylene vinylene) (DP-PPV-PEO) into the nanopores of polystyrene templates prepared by the self-assembly of polylactide-containing block copolymers after pyrolysis [58]. Hydrophilic DP-PPV-PEO polymers with different lengths of PEO segment were synthesized via a modified Gilch route. The polymers were successfully introduced into the nanoporous template by a solvent-annealing process, and well-defined polymer nanostructures were generated.

Different from a DP-PPV-PEO thin film, the emission of the templated polymer arrays was significantly enhanced [58]. By studying the grazing incidence Fourier transform infrared (GI-FTIR) and polarized photoluminescence (PL) spectroscopy, the enhancement was found to be caused by the better chain alignment of the PPV backbone, which is driven by the nanoscale spatial effect of the template polymers. Therefore, the self-quenching of the polymer luminescence is sharply reduced. The nanoscale spatial effect is illustrated in Fig. 7 [58]. DP-PPV-PEO chains are filled into the nanopores of the polymer templates by solvent annealing, and the polymer chains are oriented parallel to the cylindrical direction of the nanopores.

6. Other applications of DP-PPV and DP-PPV derivatives

Most DP-PPV and DP-PPV derivatives are used for the applications of organic light-emitting diodes. Additionally, they can be used for other applications such as dielectrics or chemosensors [64,65].

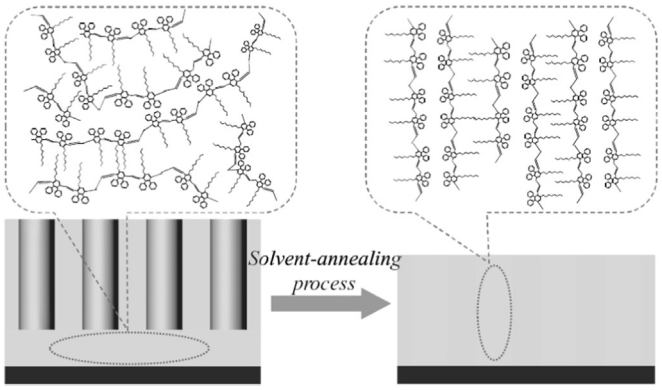

Fig. 7. Illustration of chain alignment from DP-PPV-PEO film induced by the solvent annealing process. Reproduced with permission from the literature [58].

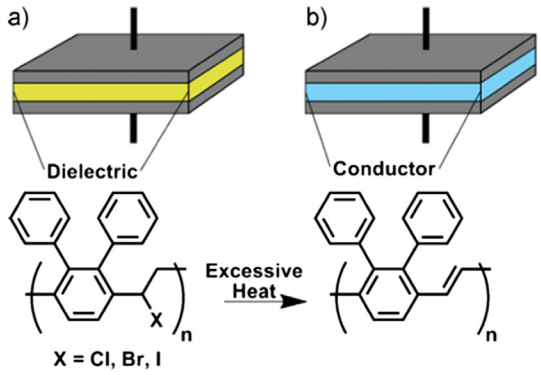

Fig. 8. Precursor polymers (a) can function as dielectric materials until excessive heats eliminate the halide and convert the polymers to conjugated states (b). Reproduced with permission from the literature [64].

6.1. DP-PPV for developing dielectric materials

Precursor DP-PPV polymers can be used as dielectric materials that can fail as a short by conjugating at higher temperatures. Johnson et al. studied that precursor polymers can function as dielectric materials until excessive heats eliminate the halide and convert the polymers to conjugated states, as shown in Fig. 8 [64]. The charging of capacitors can therefore be prevented, and a fundamental safety mechanism for high-voltage electrical devices can be provided. They investigated the synthesis and characterization of two DP-PPV precursor polymers that use bromo and iodo leaving groups, which can efficiently switch the polymers to conjugated states over a range of temperatures [64]. Even though chloro precursor polymers have good dielectric properties, conjugation of the DP-PPV polymer backbones can cause failure of the capacitors once the preset temperature are reached.

Electrical measurements of polymer thin film capacitors prepared from the chloro DP-PPV precursor polymers to determine the dielectric constant (k) and the dissipation factor (DF) at varying frequencies have also been studied [64]. Fig. 9a and b show the results of capacitance and DF values of chloro DP-PPV polymers on 6 different areas of the polymer film at 1 V and frequencies of 20 Hz, 100 Hz, 1 KHz, 10 KHz, 100 KHz, and 1 MHz. The average dielectric constant was observed to be ~4.2, significantly higher than other non-fluorinated polymer dielectrics [66]. The high dielectric constant is caused by the significant polarizability of the polymer structure. The performance of the polymers as capacitors at elevated temperatures has also been studied (see Fig. 9c, d). Both the capacitance and the DF values increased significantly and then decreased after reaching 200 °C.

6.2. DP-PPV derivatives for chemosensor applications

DP-PPV derivatives can also been used for chemosensor applications to detect explosive compounds such as 2,6-dinitrotoluene

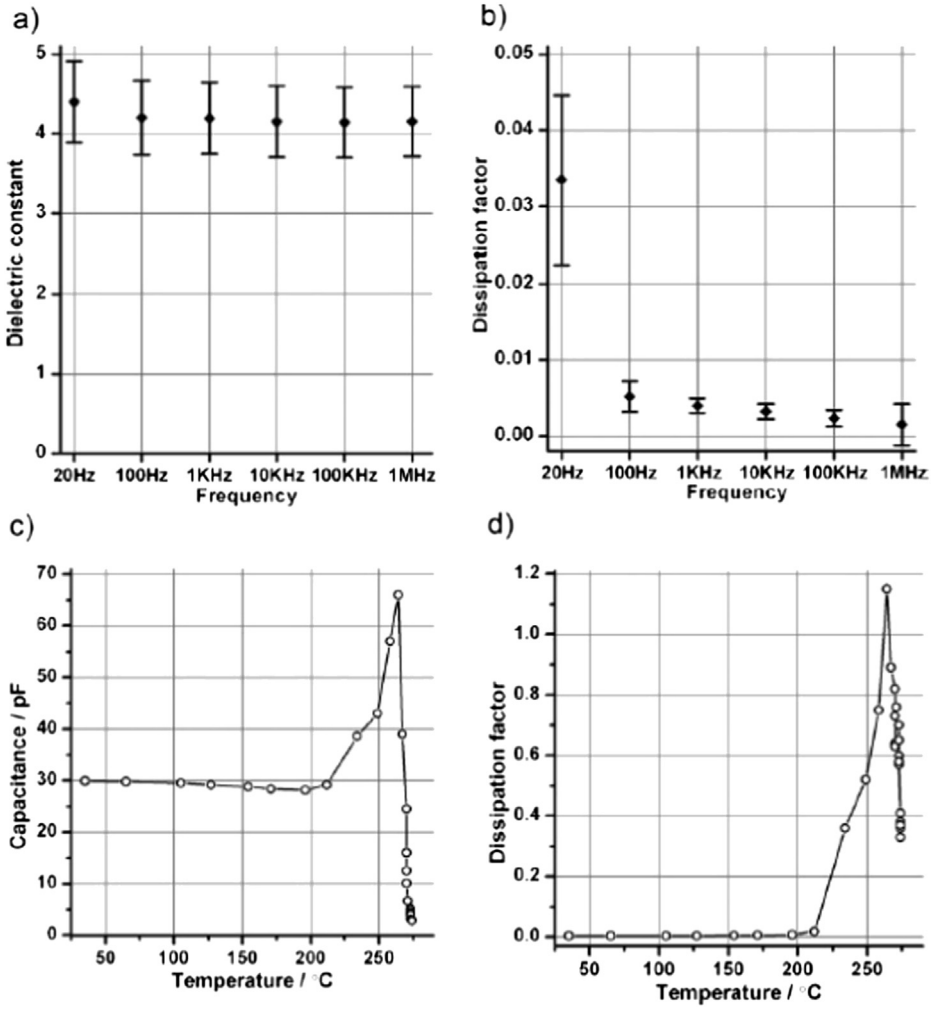

Fig. 9. Electrical measurements of polymer thin film capacitors prepared from the chloro DP-PPV precursor polymers. Dielectric constants (a) and dissipation factors (b) at varying frequencies. c) Capacitances (c) and dissipation factors (d) as a function of temperatures. Reproduced with permission from the literature [64].

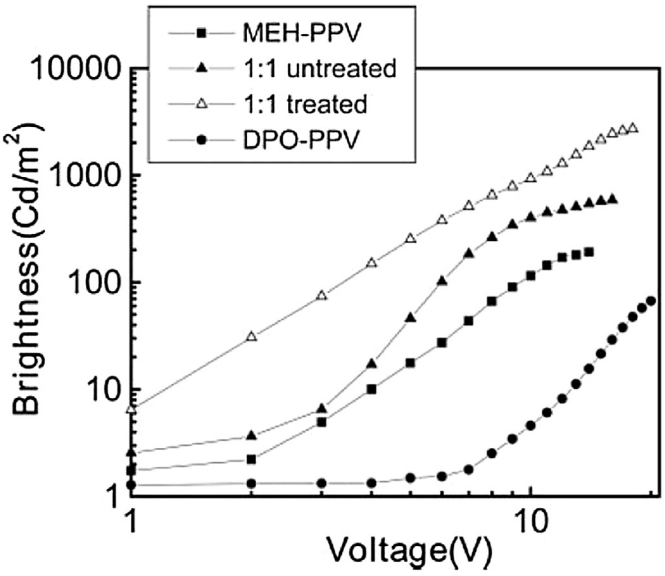

Fig. 10. Double logarithmic plots of the brightness versus the voltage for PLEDs prepared with MEH–PPV (solid square), DP8–PPV (solid circle), the blend without thermal treatment (solid triangle), and the blend with thermal treatment (empty triangle). Reproduced with permission from the literature [69].

(DNTs) or 2,4,6-trinitrotoluene (TNT). Chang et al. studied the potential use of poly(2,3-diphenyl-5-n-decyl-p-phenylene vinylene) (DP10-PPV) as chemosensors [65]. Thin films of DP10-PPV were deposited on cover glasses by spin coating and were placed under vacuum before use. The polymer film was then exposed to the vapor of an analyte in a sealed vial at room temperature. Upon exposing to vapor of analytes such as TNT, rapid photoluminescence quenching was observed. For instance, DP10-PPV shows 19% quenching by TNT in 10 s. It was observed that the polymer thin films exhibited relatively strong fluorescent quenching by exposing to all the nitro analytes. But relatively weak response was detected to 1,4-benzoquinone (BQ) even after exposing for longer periods of time. DP10-PPV shows 9.3 and 18% quenching by exposing to BQ for 1 and 10 min, respectively.

The fluorescent quenching of DP10-PPV can be attributed to many factors. One factor is the permeability P, which is determined mainly by the analyte solubility in the polymer. The analyte solubility can be predicted by the solubility parameters of the analyte and the polymer. The solubility parameters of DP10-PPV associated with dispersion force, polar forces, and hydrogen bonding were calculated to be 17.8, 0.5, and 0 $(J/mL)^{1/2}$, by using the group-contribution method. The predicted analyte solubility in the polymer does not agree well with the fluorescent quenching results, implying that there are other dominant factors than solubility parameters. The fluorescence quenching by analytes is also dependent on factors such as the interchain charge transfer and the binding strength between polymers and analytes. These factors can be considered in an attempt to prepare more sensitive and efficient polymers for TNT chemosensors.

7. Blends of DP-PPV derivatives and other materials

When DP-PPV derivatives are blended with other polymers, energy transfer might occur. Dogariu et al. studied the dynamics of Forster energy transfer from host polymers with larger gap (DP6-PPV) to guest polymers with smaller gap (poly 2,5-bis(2′-ethylhexoxy.-1,4-phenyleneviny-lene) (BEH-PPV) by using subpicosecond spectroscopy and pump–probe experiments [67]. The ultrafast pump-probe and spectral measurements on the stimulated emission (SE) and photoinduced absorption (PA) showed that 10–20 ps are necessary for complete energy transfer, depending on the concentration density of the guest molecules. From the energy transfer rates, the Forster interaction range was calculated to be 3–4 nm, which is 1.4 times longer than the theoretical values from the spectral overlap. The difference was attributed to the delocalization of the excited states.

The commonly used poly(2-methoxy-5-(2′-ethyl-hexyloxy)-p-phenylene vinylene) (MEH-PPV) has also been used to blend with DP-PPV derivatives to study the miscibility and device performance. Chou et al. investigated the miscibility and luminescence properties of MEH-PPV/DP8-PPV [68]. As measured by fluorescence spectroscopy and differential scanning calorimetry, MEH-PPV and DP8-PPV are basically immiscible, resulting in insufficient energy transfer from DP8-PPV to MEH-PPV. The turn-on voltages of the PLED devices of the polymer blends were lower than those of their pristine polymers, but the EL quantum efficiencies of the polymer blends were higher. The EL results indicate that the majority of the EL emission was from the MEH-PPV, and the DP8-PPV only played a supporting role to improve the emission efficiency of MEH-PPV.

Chow et al. later observed that the EL properties of the MEH-PPV/DP8-PPV blend can be significantly improved after a thermal treatment [69,70]. Fig. 10 shows the double logarithmic plots of the brightness versus the forward bias for PLED devices prepared from different samples. After a thermal treatment at 200 °C for 2 h in vacuum, the maximum brightness can reach 2700 cd/m^2 at 18 V. The EL quantum yield for the thermally treated blend was also improved to 2 cd/A, ~10 times higher than that of MEH–PPV (~0.21 cd/A). The authors proposed that the broken MEH-PPV chain segments were able to chemically bond to the DP8-PPV by transvinylation after thermal treatment [68,69]. The chemical bonding converted the immiscible MEH-PPV/DP8-PPV blends into vertically segregated structures similar to block copolymers. In the segregated structure, both the HOMO and LUMO levels of the MEH-PP were higher than those of DPO-PPV. Therefore, the charges were easily captured in the heterojunction regions, resulting in the improvement of the EL quantum efficiencies and stability of the devices.

8. Conclusion

In conclusion, we have reviewed the synthesis and characterization of several examples of DP-PPV derivatives, one of the most studied representatives in the PPV series. Various substituents can be introduced to the polymers to modify their properties. For example, long alkyl chains can be incorporated to improve the solubility of the polymers. Liquid crystalline side chains can also be incorporated to achieve polarized emissions. By introducing dendritic side groups, the quantum efficiency of the device was greatly enhanced. Charge transport groups can also be integrated on the pendant phenyl ring to decrease the driving voltage of the PLED devices. By incorporating methoxy or long branched alkoxy chains into DP-PPV, a maximum luminance of 78,050 cd/m^2 with a low turn-on voltage of 4.0 V was also achieved by fabricating multilayer electroluminescent devices. The photophysics, self-assembly behaviors, and confinement-induced property changes of DP-PPV derivatives are also discussed. Finally, applications of DP-PPV derivatives in areas such as dielectric materials or chemosensors are reviewed.

Acknowledgment

This work was supported by the National Science Council.

References

[1] Burroughes JH, Bradley DDC, Brown AR, Marks RN, Mackay K, Friend RH, et al. Nature 1990;347(6293):539–41.

[2] Friend RH, Gymer RW, Holmes AB, Burroughes JH, Marks RN, Taliani C, et al. Nature 1999;397(6715):121–8.
[3] Brabec CJ, Sariciftci NS, Hummelen JC. Advanced Functional Materials 2001;11(1):15–26.
[4] Greenham NC, Moratti SC, Bradley DDC, Friend RH, Holmes AB. Nature 1993;365(6447):628–30.
[5] Ho PKH, Kim JS, Burroughes JH, Becker H, Li SFY, Brown TM, et al. Nature 2000;404(6777):481–4.
[6] Cao Y, Parker ID, Yu G, Zhang C, Heeger AJ. Nature 1999;397(6718):414–7.
[7] Grice AW, Bradley DDC, Bernius MT, Inbasekaran M, Wu WW, Woo EP. Applied Physics Letters 1998;73(5):629–31.
[8] Sirringhaus H, Tessler N, Friend RH. Science 1998;280(5370):1741–4.
[9] Blom PWM, Vissenberg M. Materials Science & Engineering R Reports 2000;27(3–4):53–94.
[10] Son S, Dodabalapur A, Lovinger AJ, Galvin ME. Science 1995;269(5222): 376–8.
[11] Mitschke U, Bauerle P. Journal of Materials Chemistry 2000;10(7):1471–507.
[12] Bernius MT, Inbasekaran M, O'Brien J, Wu WS. Advanced Materials 2000;12(23):1737–50.
[13] Grimsdale AC, Chan KL, Martin RE, Jokisz PG, Holmes AB. Chemical Reviews 2009;109(3):897–1091.
[14] Nguyen TQ, Martini IB, Liu J, Schwartz BJ. Journal of Physical Chemistry B 2000;104(2):237–55.
[15] Neef CJ, Ferraris JP. Macromolecules 2000;33(7):2311–4.
[16] Scott JC, Kaufman JH, Brock PJ, DiPietro R, Salem J, Goitia JA. Journal of Applied Physics 1996;79(5):2745–51.
[17] Hu DH, Yu J, Barbara PF. Journal of the American Chemical Society 1999;121(29):6936–7.
[18] Yeh WL, Chen HL, Chen SA. Synthetic Metals 2007;157(10–12):407–13.
[19] Hsieh BR, Feld WA. Polymer Preprints 1993;34(2):410–1.
[20] Hsieh BR, Antoniadis H, Bland DC, Feld WA. Advanced Materials 1995;7(1):36–8.
[21] Hsieh BR, Wan WC, Yu Y, Gao YL, Goodwin TE, Gonzalez SA, et al. Macromolecules 1998;31(3):631–6.
[22] Wan WC, Antoniadis H, Choong VE, Razafitrimo H, Gao Y, Feld WA, et al. Macromolecules 1997;30(21):6567–74.
[23] Lee HG, Kim S, Hwang C, Choong V, Park Y, Gao Y, et al. Journal of Applied Physics 1997;82(10):4962–5.
[24] Razafitrimo H, Gao Y, Feld WA, Hsieh BR. Synthetic Metals 1996;79(2):103–6.
[25] Antoniadis H, Roitman D, Hsieh B, Feld WA. Polymers for Advanced Technologies 1997;8(7):392–8.
[26] Ettedgui E, Razafitrimo H, Gao Y, Hsieh BR, Feld WA, Ruckman MW. Physical Review Letters 1996;76(2):299–302.
[27] Hsieh BR, Yu Y, Forsythe EW, Schaaf GM, Feld WA. Journal of the American Chemical Society 1998;120(1):231–2.
[28] Li AK, Yang SS, Jean WY, Hsu CS, Hsieh BR. Chemistry of Materials 2000;12(9): 2741–4.
[29] Yang SH, Chen SY, Wu YC, Hsu CS. Journal of Polymer Science Part A Polymer Chemistry 2007;45(15):3440–50.
[30] Yang SH, Hsu CS. Journal of Polymer Science Part A-Polymer Chemistry 2009;47(11):2713–33.
[31] Yang SH, Li HC, Chen CK, Hsu CS. Journal of Polymer Science Part A-Polymer Chemistry 2006;44(23):6738–49.
[32] Chen KB, Li HC, Chen CK, Yang SH, Hsieh BR, Hsu CS. Macromolecules 2005;38(21):8617–24.
[33] Liao YM, Shih HM, Hsu KH, Hsu CS, Chao YC, Lin SC, et al. Polymer 2011;52(17):3717–24.
[34] Yang SH, Chen JT, Li AK, Huang CH, Chen KB, Hsieh BR, et al. Thin Solid Films 2005;477(1–2):73–80.
[35] Louwet F, Vanderzande D, Gelan J, Mullens J. Macromolecules 1995;28(4):1330–1.
[36] Huang Y, Lu ZY, Peng Q, Xie RG, Xie MG, Peng JB, et al. Journal of Materials Science 2005;40(3):601–4.
[37] Watanabe Y, Mihara T, Koide N. Macromolecules 1997;30(6):1857–9.
[38] Akagi K, Oguma J, Shibata S, Toyoshima R, Osaka I, Shirakawa H. Synthetic Metals 1999;102(1–3):1287–8.
[39] Kijima M, Akagi K, Shirakawa H. Synthetic Metals 1997;84(1–3):237–8.
[40] Bao ZN, Amundson KR, Lovinger AJ. Macromolecules 1998;31(24):8647–9.
[41] Chou CH, Shu CF. Macromolecules 2002;35(26):9673–7.
[42] Jakubiak R, Bao Z, Rothberg L. Synthetic Metals 2000;114(1):61–4.
[43] Yu LS, Chen SA. Synthetic Metals 2002;132(1):81–6.
[44] Fu DK, Xu B, Swager TM. Tetrahedron 1997;53(45):15487–94.
[45] Chang SM, Su PK, Lin GJ, Wang TJ. Synthetic Metals 2003;137(1–3):1025–6.
[46] Chiu CC, Lin KF, Chou HL. Journal of Polymer Science Part A-Polymer Chemistry 2003;41(14):2180–6.
[47] Renaud C, Josse Y, Lee CW, Nguyen TP. Journal of Materials Science-Materials in Electronics 2008;19:S87–91.
[48] Polyakov VI, Rossukanyi NM, Rukovishnikov AI, Pimenov SM, Karabutov AV, Konov VI. Journal of Applied Physics 1998;84(5):2882–9.
[49] Li YC, Chen KB, Chen HL, Hsu CS, Tsao CS, Chen JH, et al. Langmuir 2006;22(26):11009–15.
[50] Li YC, Chen CY, Chang YX, Chuang PY, Chen JH, Chen HL, et al. Langmuir 2009;25(8):4668–77.
[51] Liao SC, Lai CS, Yeh DD, Rahman MH, Hsu CS, Chen HL, et al. Reactive & Functional Polymers 2009;69(7):498–506.
[52] Lukyanov A, Malafeev A, Ivanov V, Chen HL, Kremer K, Andrienko D. Journal of Materials Chemistry 2010;20(46):10475–85.
[53] Wu YC, Ren XK, Chen EQ, Lee HM, Duvail JL, Wang CL, et al. Macromolecules 2012;45(11):4540–9.
[54] Ren XK, Wu YC, Wang SJ, Jiang SD, Zheng JF, Yang S, et al. Macromolecules 2013;46(1):155–63.
[55] Dogariu A, Heeger AJ, Wang HL. Physical Review B 2000;61(23):16183–6.
[56] Mehata MS, Hsu CS, Lee YP, Ohta N. Journal of Physical Chemistry C 2012;116(28):14789–95.
[57] Qi DF, Kwong K, Rademacher K, Wolf MO, Young JF. Nano Letters 2003;3(9):1265–8.
[58] Lo KH, Ho RM, Liao YM, Hsu CS, Massuyeau F, Zhao YC, et al. Advanced Functional Materials 2011;21(14):2729–36.
[59] Chen JT, Hsu CS. Polymer Chemistry 2011;2(12):2707–22.
[60] Zhang MF, Dobriyal P, Chen JT, Russell TP, Olmo J, Merry A. Nano Letters 2006;6(5):1075–9.
[61] McCutcheon MW, Young JF, Pattantyus-Abraham AG, Wolf MO. Journal of Applied Physics 2001;89(8):4376–9.
[62] Thurn-Albrecht T, Schotter J, Kastle CA, Emley N, Shibauchi T, Krusin-Elbaum L, et al. Science 2000;290(5499):2126–9.
[63] Zhang MF, Yang L, Yurt S, Misner MJ, Chen JT, Coughlin EB, et al. Advanced Materials 2007;19(12):1571.
[64] Johnson RS, Cicotte KN, Mahoney PJ, Tuttle BA, Dirk SM. Advanced Materials 2010;22(15):1750.
[65] Chang CP, Chao CY, Huang JH, Li AK, Hsu CS, Lin MS, et al. Synthetic Metals 2004;144(3):297–301.
[66] Takahagi T, Saiki A, Sakaue H, Shingubara S. Japanese Journal of Applied Physics Part 1-Regular Papers Short Notes & Review Papers 2003;42(1):157–61.
[67] Dogariu A, Gupta R, Heeger AJ, Wang H. Synthetic Metals 1999;100(1):95–100.
[68] Chou HL, Lin KF, Wang DC. Journal of Polymer Research 2006;13(1):79–84.
[69] Chow HL, Lin KF, Wang DC. Journal of Polymer Science Part B Polymer Physics 2006;44(1):62–9.
[70] Lin KF, Fan YL, Chow HL. Polymer International 2006;55(8):938–44.

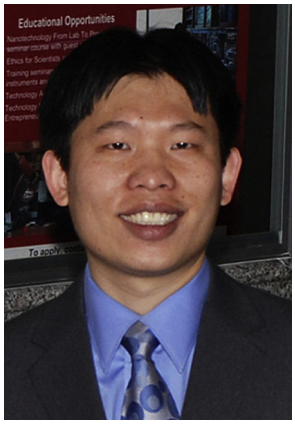

Jiun-Tai Chen received his B.S. degree in 1999 and M.S. degree in 2001 from the Department of Applied Chemistry at National Chiao Tung University. He joined Prof. Thomas Russell's group in 2003 and completed his Ph.D. in 2008 at the University of Massachusetts, Amherst in Polymer Science and Engineering, where his thesis work focused on template-based nanomaterials. He then joined the Center for Nano- and Molecular Science and Technology at the University of Texas at Austin with Prof. Paul F. Barbara as a postdoctoral fellow, where he worked on electrogenerated chemiluminescence of conjugated polymers. In the summer of 2010, he joined the Department of Applied Chemistry at National Chiao Tung University as an assistant professor. His research interests include the fabrication and characterization of polymer nanomaterials for optoelectronic applications.

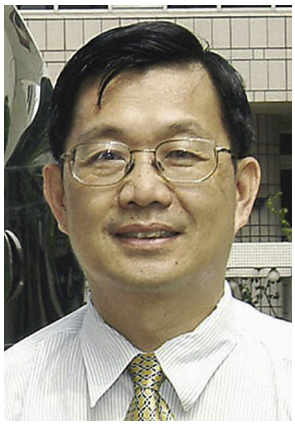

Chain-Shu Hsu received his Ph.D. degree from Case Western Reserve University in 1987 and conducted his postdoctoral work at the National Tsing Hua University in Taiwan. He joined the Department of Applied Chemistry of the National Chiao Tung University, Taiwan, in 1988 as an associate professor and was promoted to full professor in 1991. Currently he is serving as a vice president and chair professor of the National Chiao Tung University. His research interests include liquid crystalline polymers and conjugated polymers, polymer light-emitting diodes, and organic solar cells. He has published more than 200 research papers and 20 patents. He is currently on the international advisory board of Polymer and editorial boards of the Journal of Polymer Science, Polymer Chemistry, and the Journal of Polymer Research. He received the Excellent Research Award of the National Science Council, Taiwan, in 1994, the Franco-Taiwan Scientific Award for nanomaterials in 2006, Teco and Hou Chin Tui Awards in 2007, the Academic Award of Ministry of Education in 2008, and the Nanotechnology Award of Ministry of Economic Affair, Taiwan, in 2011.